NUMERICAL STUDY ON AIR-CONDITIONED INDOOR AIRFLOW BY DYNAMIC LARGE EDDY SIMULATION

Ping HE[1], Ryouichi KUWAHARA[1] and Kunio MIZUTANI[1]
[1]Tsukuba Research Institute, Sanken Setsubi Kogyo Co., Ltd., JAPAN

ABSTRACT

The aim of this research is to apply dynamic Large Eddy Simulation (LES) to predicting the complex turbulent flow field in an air-conditioned room. LES is a method to calculate turbulent flows where only the small-scale (subgrid-scale) motions are modeled and the large-scale (grid-scale) motions are computed directly. Recently, a dynamic subgrid-scale model has been developed that can evaluate a model coefficient dynamically. This paper presents a numerical simulation of LES with a dynamic mixed subgrid-scale model of a flow field in an air-conditioned room model. A full-scale model experiment is also carried out for comparison with the computational results. The distribution of the velocity field is measured with a three-dimensional ultrasonic anemometer. Good agreement between the computational and experimental results is found for time-averaged velocity and Reynolds stress.

INTRODUCTION

In recent years, Computational Fluid Dynamics (CFD) has been widely used in the field of Heating, Ventilating and Air-conditioning (HVAC). It is mainly used for designing air-conditioning systems, which require control of indoor airflow, such as in large enclosed areas and clean rooms. CFD has also been applied to the design of centralized air-conditioning systems, such as in office buildings, in order to achieve a comfortable indoor thermal environment. Since indoor airflow distribution and temperature distribution can be predicted before constructing an air-conditioning system, CFD is used for the design and planning stages of air-conditioning systems. Moreover, CFD is a very useful tool for examining design changes at the construction site of an air-conditioning system. In connection with the spread of CFD technology, there is demand for improved analysis accuracy, which requires a highly precise turbulence model. However, the flow field in an air-conditioned room involves complicated turbulence; since the supplied airflow can be either cold air or warm air, the effect of buoyancy is strong and numerical analysis by CFD is difficult. The k-ε two-equation turbulence model most widely used for the numerical analysis of a turbulent flow in the field of engineering has limited prediction accuracy when applied to such flow fields as indoor airflow. Another approach to modeling a turbulent flow is Large Eddy Simulation (LES) [1]. Turbulence models based on Reynolds-averaged equations such as the k-ε two-equation model can resolve only the flow field, which is averaged over time. In LES, the large-scale flow field obtained by the space average is directly simulated, and only the small-scale influences are modeled. Therefore, LES simulates a time-dependent flow field and can obtain detailed information of turbulence flow. The weak points of LES are that it needs a large amount of calculation time and the calculation tends to become unstable. The research on LES is increasing with the rapid advances in

computer technology. Recently, Germano et al. [2] developed a dynamic subgrid-scale model that can evaluate a model coefficient dynamically, and its prediction accuracy has been verified by Direct Numerical Simulation (DNS) and by experiment [3][4]. A mixed model has also been developed that combined the Bardina [5] model with the Smagorinsky model [1], and this model was found to dissipate energy and predict turbulence statistics better than the Smagorinsky model alone. Zang et al. [6] also proposed a dynamic mixed subgrid-scale model that was modified from the dynamic subgrid-scale model by employing the mixed model as the base model. However, there have been very few analyses of dynamic LES applied to the flow field in an air-conditioned room [7]. Therefore, the aim of this work is to achieve such an application. This paper is the first stage of this work, where an isothermal flow field in an air-conditioned room is analyzed by LES with a dynamic mixed subgrid-scale model. Moreover, a full-scale model experiment has been carried out and its results were compared with the computational results.

OUTLINE OF MODEL EXPERIMENT

Figure 1 shows the full-scale model room used for the numerical analysis and model experiment in this paper. The indoor space is 7405 *mm* in height, 3515 *mm* in width and 4910 *mm* in depth. The x_1, x_2 and x_3 directions will be referred to as the streamwise, spanwise and vertical directions, respectively. The height of a supply opening is 3410 *mm*, and the exhaust openings are set in the lower part of the opposite wall. The airflow rate of air supply is 578.11 m^3/h, and the temperature of supplied air is the same as room temperature. It is assumed to be an air-conditioning system for a space in an atrium occupied by people. In the model experiment, air velocity distributions of the vertical section in the center of the x_2 direction are measured by a three-dimensional ultrasonic anemometer. The number of measurement points was 9 x 16 in the x_1 and x_3 directions. Vertical direction traverse equipment, which can move a maximum distance of 7500 *mm* in the height direction, is used for moving the anemometer to the measurement point. The air velocities were measured at a sampling rate of 9 *Hz*, and the number of samples taken at each point was 1000. The mean air velocities and Reynolds stress were calculated by the fluctuation data.

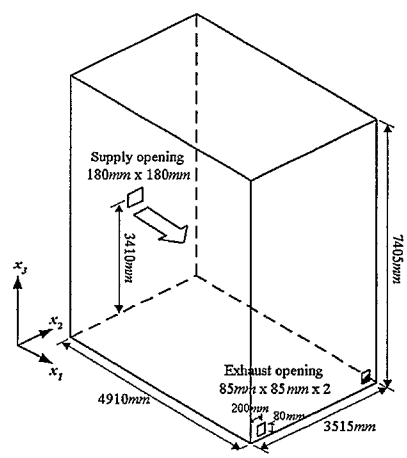

Figure 1. Room model

OUTLINE OF NUMERICAL ANALYSIS

a. Subgrid-scale model

Table 1 shows the basic equations of the dynamic mixed subgrid-scale model used for LES in this study. The SGS stress τ_{ij} is expressed as Eq. (3) by the Smagorinsky model and the Bardina model. Term L_{mij} in the right side of Eq. (3) is defined by the Bardina model. In the Smagorinsky model, the sum of cross term and Leonard term is assumed to be zero, and only the subgrid-scale Reynolds stress is modeled. The mixed model calculates the Leonard term and models the cross term and the subscale-grid

Table 1. Basic governing equations

$$\frac{\partial \bar{u}_j}{\partial x_j}=0 \quad (1)$$

$$\frac{\partial \bar{u}_i}{\partial t}+\frac{\partial \bar{u}_i \bar{u}_j}{\partial x_j}=-\frac{1}{\rho}\frac{\partial \bar{p}}{x_i}+\frac{\partial}{\partial x_j}\left(\nu\frac{\partial \bar{u}_i}{\partial x_j}\right)-\frac{\partial \tau_{ij}}{\partial x_j} \quad (2)$$

$$\tau_{ij}-\frac{1}{3}\tau_{kk}=-2C\bar{\Delta}^2|\bar{S}|\bar{S}_{ij}+L_{ij}^m-\frac{1}{3}\delta_{ij}L_{kk}^m \quad (3)$$

$$L_{ij}^m=\overline{\bar{u}_i\bar{u}_j}-\bar{u}_i\bar{u}_j \quad (4)$$

$$C=-\frac{1}{2}\frac{(L_{ij}-H_{ij})M_{ij}}{M_{ij}^2} \quad (5)$$

$$L_{ij}=\widetilde{u_iu_j}-\tilde{u}_i\tilde{u}_j \quad (6) \qquad M_{ij}=\tilde{\Delta}^2|\tilde{S}|\tilde{S}_{ij}-\bar{\Delta}^2\widetilde{|S|S_{ij}} \quad (7)$$

$$H_{ij}=(\widetilde{u_iu_j}-\tilde{u}_i\tilde{u}_j)-(\widetilde{u_iu_j}-\tilde{u}_i\tilde{u}_j) \quad (8)$$

$$\bar{S}_{ij}=\frac{1}{2}\left(\frac{\partial \bar{u}_i}{\partial x_j}+\frac{\partial \bar{u}_j}{\partial x_i}\right) \quad (9) \qquad |\bar{S}|=(\bar{S}_{ij}\bar{S}_{ij})^{1/2} \quad (10)$$

$$\tilde{S}_{ij}=\frac{1}{2}\left(\frac{\partial \tilde{u}_i}{\partial x_j}+\frac{\partial \tilde{u}_j}{\partial x_i}\right) \quad (11) \qquad |\tilde{S}|=(\tilde{S}_{ij}\tilde{S}_{ij})^{1/2} \quad (12)$$

$$\bar{f}^n=\left(1-\frac{\Delta\tau}{T}\right)\bar{f}^{n-1}+\frac{\Delta\tau}{T}\bar{f}^n \quad (13)$$

Table 2. Boundary conditions

Inflow boundary	$U_1=4.9563$ *m/s*
Outflow boundary	$U_1=11.1132$ *m/s*,
Wall boundary	$u_i^+=x_n^+, (x_n^+ \leqq 11.81)$
	$u_i^+=A(x_n^+)^B, (x_n^+ > 11.81)$
	$A=8.3, B=1/7$

Reynolds stress. The modeling in the dynamic mixed model is based on the dynamic procedure suggested by Germano et al. The model coefficient C in Eq. (3) is equivalent to the square of original model coefficient Cs in the Smagorinsky model. In the actual implementation, the model coefficient C is calculated locally with a least-square approach suggested by Lilly [8]. In addition, Term H_{ij} in the right side of Eq. (5), which is similarly defined by the Bardina model, is obtained by the formulations of Vreman et al. [9]. Taylor's series expansion is employed to obtain the test-scale filter and the twice-filter. Since there is no homogeneous direction for averaging the model coefficient C in the flow field of the present work, we used a time filter as Eq. (13) to prevent the analysis from failure. Here, f_n is the C at the time step n of calculation, T is a time scale, Dt is a time interval, and $Dt/T = 10^{-3}$. Moreover, previous work showed that if the locally computed C is negative, the analysis will become unstable. To guarantee that this does not happen, C is set to zero whenever it becomes negative.

b. Numerical method

The indoor space of the full-scale model used as the computational domain is the same as that of the experiment. The size of the grid system is 33 x 54 x 59 (x_1, x_2, x_3 directions, respectively) cells. The grid spacing is expanded and contracted in all directions, and the minimum value of grid spacing near the walls is 30 *mm*. The variables of numerical analysis are stored on a staggered mesh. The Piacsek-Williams scheme is used for the convective term and a second-order centered differential scheme is applied for the other spatial derivatives. The time marching scheme is the Adams-Bashforth scheme. The boundary conditions are shown in Table 2. The inflow boundary condition is based on experimental results. For the boundary conditions at the solid walls, a two-layer model [10] is employed. The initial condition is the velocity field computed by the k-ε two-equation model. The time interval of analysis is 10^{-3} seconds. The computation was first carried out for 60 seconds. Simulation then continued and statistics were collected during periods of 30 seconds.

RESULTS AND DISCUSSION

a. Mean velocity vector

The mean velocity vectors obtained by numerical analysis and by experiment in the vertical section at the center of the x_2 axis is shown in Fig. 2. The flow pattern by numerical analysis and that by experiment are very similar. The supplied air impinges on the downstream wall and becomes two large recirculating flows in the upper and lower parts of the model room. Furthermore, it is clear from Fig. 2 that the recirculating flow reaches the upstream wall and then combines with the supplied air around the supply opening. However, some differences in the central positions of the recirculating regions appeared between the results of the experiment and those of the calculation.

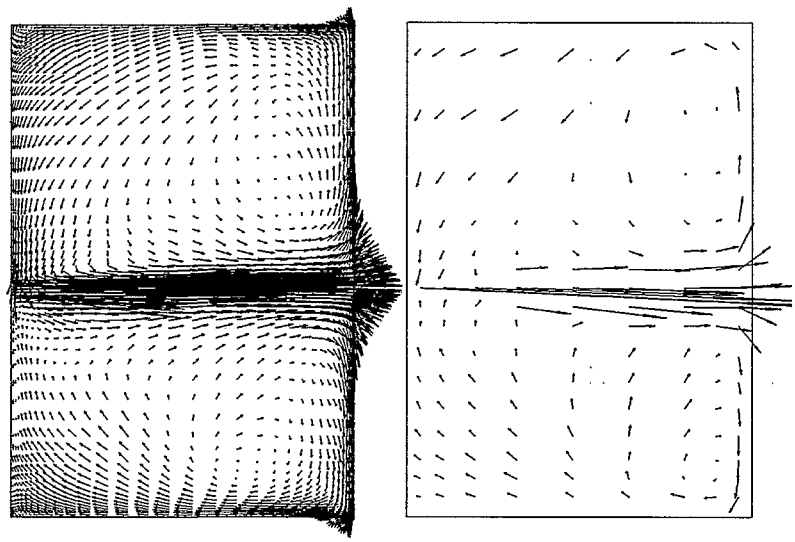

Numerical analysis Experiment

Figure 2. Comparison of mean velocity vector

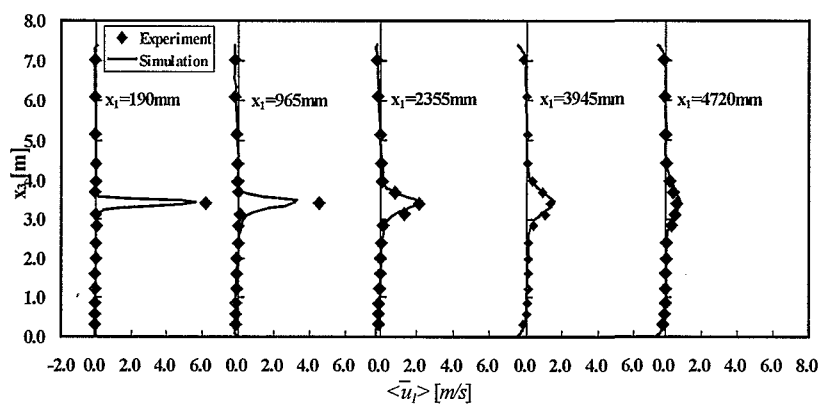

Figure 3. Comparisons of mean velocity $<\overline{u}_1>$

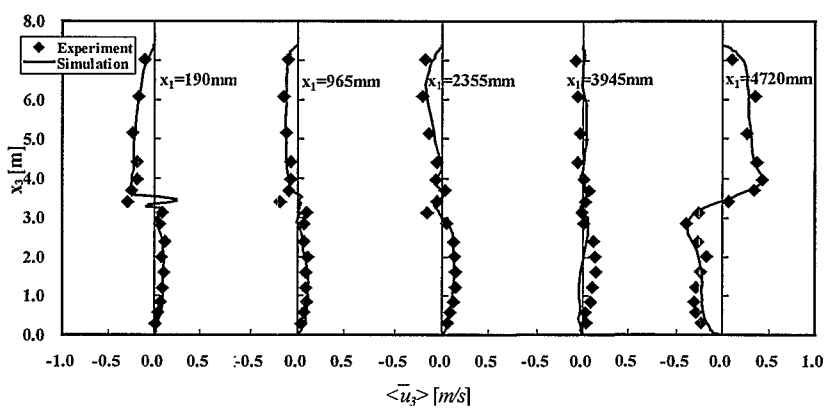

Figure 4. Comparisons of mean velocity $<\overline{u}_3>$

b. Mean velocity profile

Figures 3 and 4 show comparisons of the vertical profiles of mean velocity $<\overline{u}_1>$ and $<\overline{u}_3>$ at the center of the x_2 axis, respectively. In Fig. 3, the profiles of $<\overline{u}_1>$ predicted by numerical analysis agree well with those of the experiment except for the numerical value of maximum velocity on the upstream side of the room, where the computation underestimates the maximum value of mean velocity $<\overline{u}_1>$. This difference is related to the distribution of Reynolds stress - $<u_1'u_3'>$ and will be discussed later. In Fig. 4, the predicted and measured profiles for $<\overline{u}_3>$

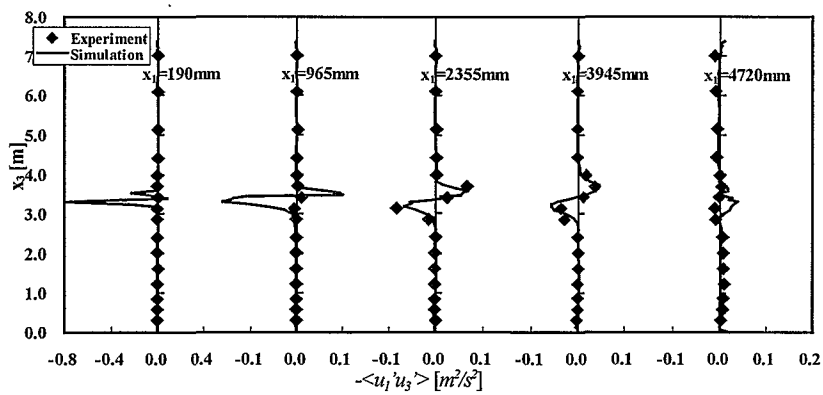

Figure 5. Comparison of Reynolds stress $-\langle u_1'u_3'\rangle$

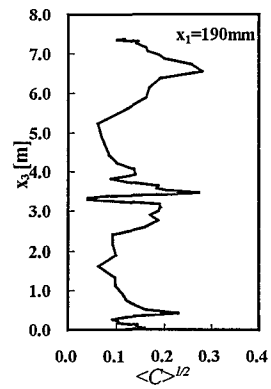

Figure 6. Vertical profile of C

also agree well with each other, although discrepancies between the simulation and experimental results are observed at $x_1 = 3945$ mm. These discrepancies of mean velocity $\langle\overline{u}_3\rangle$ were due to the aforementioned differences in the central positions of the recirculating regions. Since the computed result shows the central position of a recirculating flow in the lower region of the room near $x_1 = 3945$ mm, the predicted value of $\langle\overline{u}_3\rangle$ was lower than that of the experiment in that area.

c. Reynolds stress $-u_1'u_3'$ and model coefficient C

The vertical profiles of time-averaged Reynolds stress $-\langle u_1'u_3'\rangle$ on the centerline in the x_2 direction are plotted in Fig. 5. In the figure, the computed Reynolds stress involves the large-scale quantities resolved by the grid. On the leeward side of the room, the overall agreement of computational results with experimental results is good, while on the windward side of the room, the computation greatly overestimates the absolute value of $-\langle u_1'u_3'\rangle$ around the supply opening level. This overestimation caused the aforementioned underestimation of the peaks of $\langle\overline{u}_1\rangle$ and shows the probability that the turbulence intensity of the supplied air should be considered on the inflow boundary which was given as a constant value in this work. Figure 6 shows the vertical profile of model coefficient C obtained by simulation on the centerline in the x_2 direction and 190 mm away from the upstream wall. In this figure, C is presented as $\langle C\rangle^{1/2}$, which is equivalent to the original Smagorinsky constant Cs. The value of $\langle C\rangle^{1/2}$ becomes large near the floor level and decreases with a steep gradient.

CONCLUSIONS

The numerical approach was carried out for the prediction of flow field in an air-conditioned room by LES with the dynamic mixed subgrid-scale model. A full-scale model experiment was also carried out and compared with the computational results. The distributions of computed mean velocity show good agreement with the experimental results. However, some discrepancies of Reynolds stress between simulation and experimental results were observed, which could be due to the inflow boundary condition. While further examination still needs to be done, the present work has provided successful simulation of the complex turbulent flow field in an air-conditioned room and shows that the methodology of LES can be applied to practical air-conditioning engineering problems.

NOMENCLATURE

x_i: three components of spatial coordinate(i = 1, 2, 3: streamwise, spanwise, vertical)

u_i: velocity in i-direction

$\langle f \rangle$: time-averaged value of f

$\overline{f}$: grid-filtered value of f

f': deviation from $\langle f \rangle$, $f' = f - \langle f \rangle$

f'': deviation from $\overline{f}$, $f'' = f - \overline{f}$

Cs: Smagorinsky constant

$\overline{\Delta}_i$: grid-filter width in i-direction

$\tilde{\Delta}_i$: test-filter width in i-direction

$\overline{\Delta}$: grid-filter width, $\overline{\Delta} = \sqrt[3]{\overline{\Delta}_1 \overline{\Delta}_2 \overline{\Delta}_3}$

$\tilde{\Delta}$: test-filter width, $\tilde{\Delta} = \sqrt[3]{\tilde{\Delta}_1 \tilde{\Delta}_2 \tilde{\Delta}_3}$

u^*: friction velocity

x_n: distance from solid wall

x_n^+: $x_n^+ = \dfrac{\langle u^* \rangle x_n}{\nu}$

REFERENCES

1. Smagorinsky, J.S.: General circulation experiments with the primitive equations, part 1. Basic experiments. Monthly Weather Review, Vol.91,99. Pp99-164, 1963
2. Germano, M., Piomelli, U., Moin, P. and Cabot, W.H.: A dynamic subgrid-scale eddy viscosity model, Phys. Fluids, A3(7).pp1760-1765, 1991
3. Zang, T.A., Gilbert, N. and Kleisar, L.: Instability and Transition, pp 283 - 299,1990
4. Mochida, A., Murakami, S., Tominaga, Y., Kobayashi, H.: Large eddy simulation of turbulent vortex shedding flow past 2D square cylinder using Dynamic SGS mode (Part-1), Comparison between standard and dynamic type of Smagorinsky SGS model, Journal of Architecture, Planning and Environmental engineering, Transactions of Archi. Ins. Of Japan, No. 479, pp. 41-47, 1996 (in Japanese)
5. Bardina, J., Ferziger, J.H. and Reynolds, W.C. : Improved Subgrid-scale Models for Large Eddy Simulation, AIAA, paper-80, 1981
6. Zang, Y.; Street, R. L. and Koseff, J.R.: A dynamic mixed subgrid-scale model and its application to turbulent recirculation flows, Phys. Fluid, A5(12), pp3186-3196, 1993
7. Murakami, S., Mochida, A., Matsui, K.: Large Eddy Simulation of non-isothermal room airflow, comparison between standard and dynamic type of Smagorinsky model, Monthly Journal of Institute of Industrial Science, University of Tokyo, Vol.47,No2, pp7-12, 1995 (in Japanese)
8. Lilly, D. K.: A proposed modification of the Germano subgrid-scale closure method, Phys. Fluid, A4(3), pp633-635, 1992
9. Vreman, B., B. Geurts and H. Kuerten: On the formulation of the dynamic mixed subgrid-scale model, Phys. Fluid, 6(12), pp4057-4059, 1994
10. Werner, H. and H. Wengle: Large-eddy simulation of turbulent flow over and around a around a cube in a plate channel, Eighth symposium on turbulent shear flows, 19-4, 1991